

## Submicromolar Fluorescence ‘Turn-on’ Detection of Fluoride Anion Using *meso*-(tetra-Aryl) Calix[4]pyrrole

Anik Roy<sup>a</sup>, Ranjan Dutta<sup>\*b</sup>, Dibakar Halder<sup>a</sup>, Koushik Mandal<sup>c</sup>, Somenath Kundu<sup>d</sup>,  
Maidul Hossain<sup>d\*</sup>, Indrajit Saha<sup>\*a</sup> and Chang-Hee Lee<sup>\*e</sup>

### Supporting Information

Table of Contents	Page no.
<b>Section S1.</b> General information and instrumentation.	2
<b>Section S2.</b> Experimental section: synthetic scheme and synthetic procedures.	3-4
<b>Figure S1.</b> <sup>1</sup> H NMR spectrum of <b>1</b> in CDCl <sub>3</sub> .	5
<b>Figure S2.</b> <sup>13</sup> C NMR spectrum of <b>1</b> in CDCl <sub>3</sub> .	6
<b>Figure S3.</b> HRMS spectrum of <b>1</b>	7
<b>Figure S4.</b> <sup>1</sup> H NMR spectrum of <b>5</b> in CDCl <sub>3</sub> .	8
<b>Figure S5.</b> <sup>13</sup> C NMR spectrum of <b>5</b> in CDCl <sub>3</sub> .	9
<b>Figure S6.</b> HRMS spectrum of <b>5</b> .	10
<b>Figure S7.</b> <sup>1</sup> H NMR spectrum of <b>6</b> in CDCl <sub>3</sub> .	11
<b>Figure S8.</b> <sup>13</sup> C NMR spectrum of <b>6</b> in CDCl <sub>3</sub> .	12
<b>Figure S9.</b> HRMS spectrum of <b>6</b> .	13
<b>Section S3.</b> Experimental details for single crystal X-ray structure determination.	13
<b>Table S1.</b> Selected crystal data and refinement parameters for receptor <b>1</b> •(CH <sub>3</sub> OH) <sub>2</sub> and <b>6</b> .	14
<b>Table S2.</b> Selected crystal data and refinement parameters for <b>1</b> •CsF•CH <sub>3</sub> OH and <b>1</b> •TEAF complexes.	15
<b>Table S3.</b> Selected distances and angles for non covalent interactions seen in the single crystal X-ray structure of TEAF and CsF complexes of <b>1</b> .	16
<b>Figure S10.</b> Single crystal X-ray structure of <b>1</b> •CsF•CH <sub>3</sub> OH complex (left side) and partial view of the 1D linear supramolecular chain seen in the crystal lattice (right side).	16
<b>Figure S11.</b> Single crystal X-ray structure of <b>1</b> •TEAF complex (left side) and partial view of the 1D linear supramolecular chain seen in the crystal lattice (right side).	16
<b>Figure S12. Figure S12.</b> Differential arrangement of <i>meso</i> -aryl groups in the solid state structures of <b>1</b> •CsF•CH <sub>3</sub> OH and <b>1</b> •TEAF complexes.	17
<b>Table S4.</b> Some reported FDDA-based sensors built on calix[4]pyrrole framework for various analytes	18-19
<b>Figure S13.</b> Partial <sup>1</sup> H NMR titration spectra of receptor <b>1</b> (1.10 mM) with incremental addition of TBAF in CD <sub>3</sub> CN.	20
<b>Figure S14.</b> Partial <sup>19</sup> F NMR titration spectra of receptor <b>1</b> (3.74 mM) with incremental addition of TBAF in CD <sub>3</sub> CN.	20
<b>Figure S15.</b> Partial <sup>1</sup> H NMR titration spectra of receptor <b>1</b> (1.10 mM) with incremental addition of coumarin anion <b>2</b> <sup>-</sup> in CD <sub>3</sub> CN. Coumarin anion is used as	21

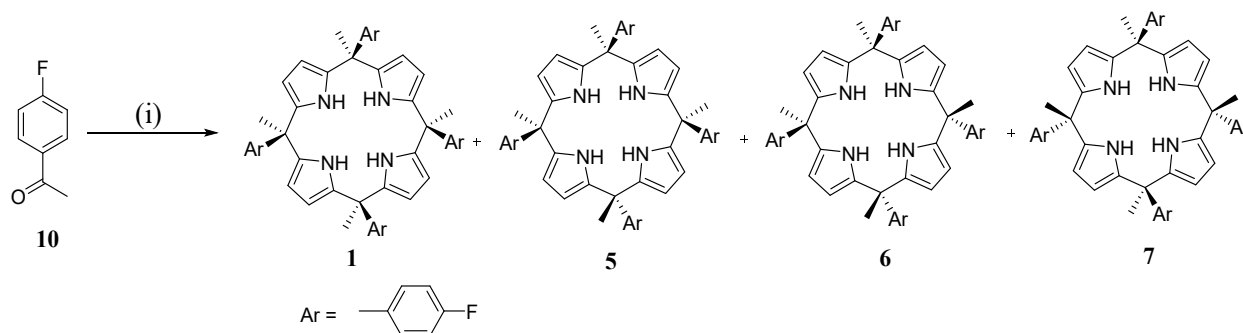
its tetrabutylammonium salt.	
<b>Figure S16.</b> <sup>1</sup> H NMR spectra of <b>1</b> ( $1.113 \times 10^{-3}$ M) in the absence and presence of coumarin anion <b>2<sup>-</sup></b> recorded in CD <sub>3</sub> CN solution.	22
<b>Figure S17.</b> Change in fluorescence intensity of <b>2<sup>-</sup></b> ( $c = 4.0 \times 10^{-6}$ M) upon incremental addition of <b>1</b> ( $c = 2.40 \times 10^{-4}$ M, 0-1.0 equivalent) in acetonitrile (left side). Change in fluorescence intensity of <b>1•2<sup>-</sup></b> ( $c = 4 \times 10^{-6}$ M) upon incremental addition of (0 – 4.0 equivalent) TBAF ( $c = 8 \times 10^{-6}$ M) in acetonitrile (right side).	23
<b>Figure S18.</b> Determination of limit of detection (L.O.D) from fluorescence titration of <b>1•2<sup>-</sup></b> with TBAF.	24
<b>Figure S19.</b> Colors of acetonitrile solution of free coumarin anion <b>2<sup>-</sup></b> , ( <b>1•2<sup>-</sup></b> ) complex, and <b>1•F<sup>-</sup></b> complex containing decomplexed <b>2<sup>-</sup></b> seen during FDDA assays under sunlight (upper panel) and UV light (lower panel). [ <b>2<sup>-</sup></b> ] = $1.3 \times 10^{-5}$ M	25
<b>Figure S20.</b> Change in fluorescence intensity of <b>1</b> ( $c = 6.4 \times 10^{-5}$ M) upon incremental addition of TBAF ( $c = 1.27 \times 10^{-2}$ M, 0-7.0 equivalent) in acetonitrile ( $\lambda_{\text{ex}} = 230$ nm).	25
<b>Figure S21.</b> ITC plot showing titration of receptor <b>1</b> (0.27 mM) with coumarin anion <b>2<sup>-</sup></b> in CH <sub>3</sub> CN at 298K.	26
<b>Figure S22.</b> ITC plot showing titration of receptor <b>1</b> (0.2 mM) with TBAF (3.76 mM) in CH <sub>3</sub> CN at 298K.	27

## Section S1. General information and instrumentation.

All chemicals and solvents were purchased from commercial sources and were used as such, unless otherwise mentioned. <sup>1</sup>H NMR spectra were recorded on 300, 400, 600 MHz Bruker NMR spectrophotometers using TMS as the internal standard. Chemical shifts are reported in parts per million (ppm). When peak multiplicities are given, the following abbreviations are used: s, singlet; br s, broad singlet; d, doublet; t, triplet; m, multiplet. <sup>13</sup>C NMR spectra were proton decoupled and recorded on 100 MHz and 75 MHz spectrometers using TMS as the internal standard. High resolution mass spectrometric (HRMS) analyses were carried out on the Agilent 6546 LC/Q-TOF instrument. Fluorescence titrations were carried out on the PerkinElmer LS 55 and Scinco FS-2 fluorescence spectrophotometer. Isothermal titration calorimetry (ITC) was performed using Nano ITC standard volume hastelloy (SVH) by TA instruments. Pyrrole was distilled at atmospheric pressure from CaH<sub>2</sub>. Fluorescence and ITC titrations were performed using HPLC grade CH<sub>3</sub>CN. Single-Crystal X-ray Crystallography Single crystal data was recorded on a Bruker AXS D8 QUEST ECO diffractometer equipped with a Mo-target rotating anode X-ray source and a graphite monochromator (Mo K $\alpha$ ,  $\lambda = 0.71073$  Å).

## Section S2. Experimental section: synthetic scheme and synthetic procedures.

### Synthetic Scheme



**Scheme 1.** Reagents and conditions: (i) pyrrole, methanesulfonic acid, methanol, 0°C to room temperature, 48h, **1** = 2%, **5** = 2.5%, **6** = 5%, **7** = not isolated

### Compounds **1**, **5**, and **6**

To a stirred solution of 4-acetylfluorobenzene **10** (2.0 g, 14.49 mmol) and pyrrole (1.07g, 0.93 mL, 15.94 mmol) in methanol (180 mL), methanesulfonic acid (0.47mL, 7.25mmol) was added under N<sub>2</sub> atmosphere at 0°C. The reaction mixture was then stirred at room temperature for 48 hours under nitrogen atmosphere. The reaction was monitored by TLC. After the completion of the reaction, the reaction mixture was quenched by saturated aqueous NaHCO<sub>3</sub> solution and extracted with DCM (2 × 300 mL). The combined organic layer was dried over anhydrous sodium sulfate and concentrated under reduced pressure. The crude reaction mixture was purified by silica-gel column chromatography using 5-7% ethylacetate/hexane (v/v) as eluent followed by re-crystallization from methanol to get the pure  $\alpha,\alpha,\beta,\beta$ -isomer **6** (540mg, 5%) as first fraction,  $\alpha\alpha\alpha\beta$ -isomer **5** (271mg, 2.5%) as second fraction and  $\alpha\alpha\alpha\alpha$ -isomer **1** (217mg, 2%) as third fraction. The isolation of  $\alpha,\beta,\alpha,\beta$ -isomer **7** was unsuccessful in our hands, presumably due to the formation of this isomer in trace amount. All the three isomeric compounds were characterized by means of <sup>1</sup>H NMR, <sup>13</sup>C NMR and HRMS spectroscopy.

Compound **1** ( $\alpha,\alpha,\alpha,\alpha$ -isomer): <sup>1</sup>H NMR (600 MHz, CDCl<sub>3</sub>):  $\delta$  7.63 (s, 4H), 7.08 – 7.04 (m, 8H), 6.91 (t,  $J$  = 8.6 Hz, 8H), 5.73 (d,  $J$  = 2.8 Hz, 8H), 1.95 (s, 12H). <sup>13</sup>C NMR (100 MHz, CDCl<sub>3</sub>):  $\delta$  161.60 (d, <sup>1</sup> $J_{C-F}$  = 244.6Hz), 143.69 (d, <sup>4</sup> $J_{C-F}$  = 3.28 Hz), 136.33, 129.09 (d, <sup>3</sup> $J_{C-F}$  = 7.68 Hz), 114.49 (d, <sup>2</sup> $J_{C-F}$  = 20.90 Hz), 106.71, 44.34, 28.08. HRMS  $m/z$  for C<sub>48</sub>H<sub>40</sub>F<sub>4</sub>N<sub>4</sub>[M+H]<sup>+</sup> calculated 749.3262, found 749.3241.

Compound **5** ( $\alpha,\alpha,\alpha,\beta$ -isomer):  $^1\text{H}$  NMR (400 MHz,  $\text{CDCl}_3$ )  $\delta$  7.45 (brs, 2H), 7.32 (s, 2H), 7.26-7.23 (m, 2H), 7.07-7.05 (m, 2H), 7.04-6.97 (m, 6H), 6.97 – 6.88 (m, 6H), 5.84-5.83 (m, 2H), 5.79-5.77 (m, 2H), 5.76-5.75 (m, 2H), 5.65-5.64 (m, 2H), 1.95 (s, 3H), 1.86 (s, 9H).  $^{13}\text{C}$  NMR (100 MHz,  $\text{CDCl}_3$ )  $\delta$  162.92, 162.79, 160.48, 160.35, 143.67, 143.63, 143.61, 143.58, 141.99, 141.96, 136.96, 136.92, 136.82, 136.50, 129.18, 129.12, 129.10, 129.06, 129.04, 128.98, 115.04, 114.83, 114.72, 114.68, 114.52, 114.48, 106.74, 106.47, 106.24, 105.85, 44.39, 44.36, 30.12, 29.16, 28.74 (note that extensive C-F coupling is seen in the proton decoupled  $^{13}\text{C}$  NMR spectrum). HRMS  $m/z$  for  $\text{C}_{48}\text{H}_{40}\text{F}_4\text{N}_4[\text{M}+\text{H}]^+$  calculated 749.3262, found 749.3244.

Compound **6** ( $\alpha,\alpha,\beta,\beta$ -isomer)  $^1\text{H}$  NMR (300 MHz,  $\text{CDCl}_3$ )  $\delta$  7.45 (brs, 4H), 7.06 – 6.99 (m, 8H), 6.95-6.89 (m, 8H), 5.93 (d,  $J = 2.7$  Hz, 4H), 5.78 (d,  $J = 2.7$  Hz, 4H), 1.90 (s, 12H).  $^{13}\text{C}$  NMR (75 MHz,  $\text{CDCl}_3$ )  $\delta$  161.58  $J = 326$  Hz, 143.13 ( $J = 4$  Hz), 136.84, 136.49, 129.01 ( $J = 11$ Hz), 114.75  $9J = 28$  Hz), 106.52, 105.99, 44.42, 29.45. HRMS  $m/z$  for  $\text{C}_{48}\text{H}_{40}\text{F}_4\text{N}_4[\text{M}+\text{H}]^+$  calculated 749.3262, found 749.3241.

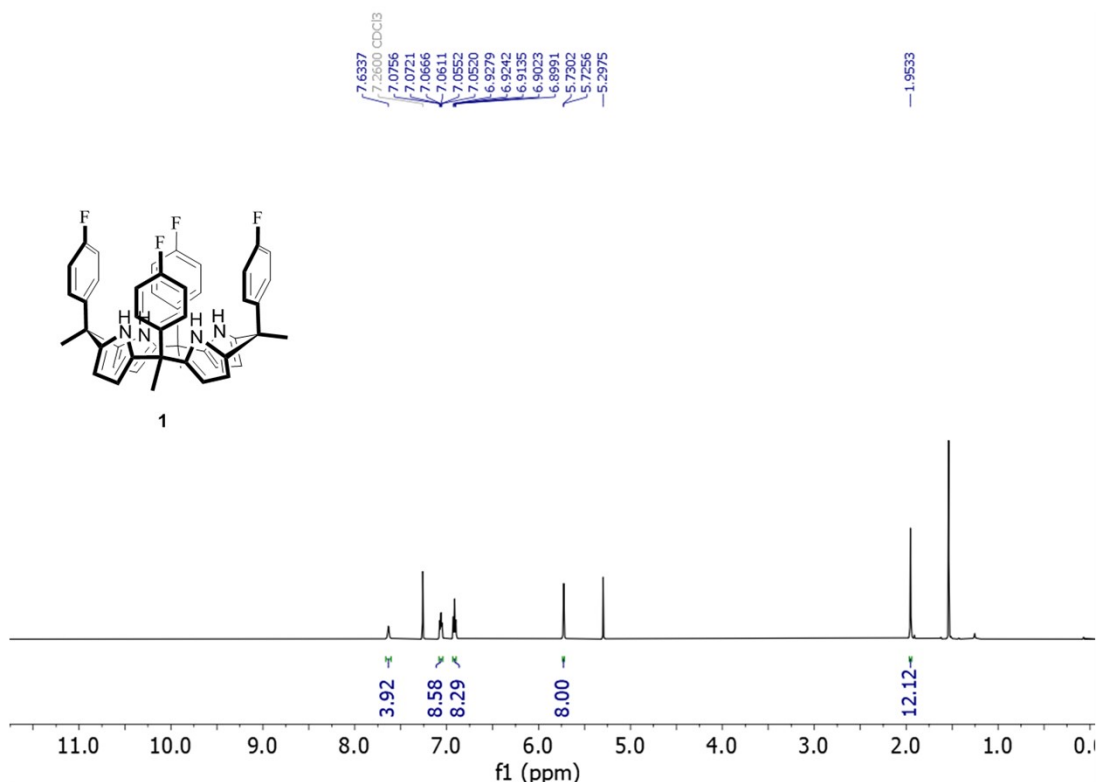


**Figure S1.**  $^1\text{H}$  NMR spectrum of **1** in  $\text{CDCl}_3$ .

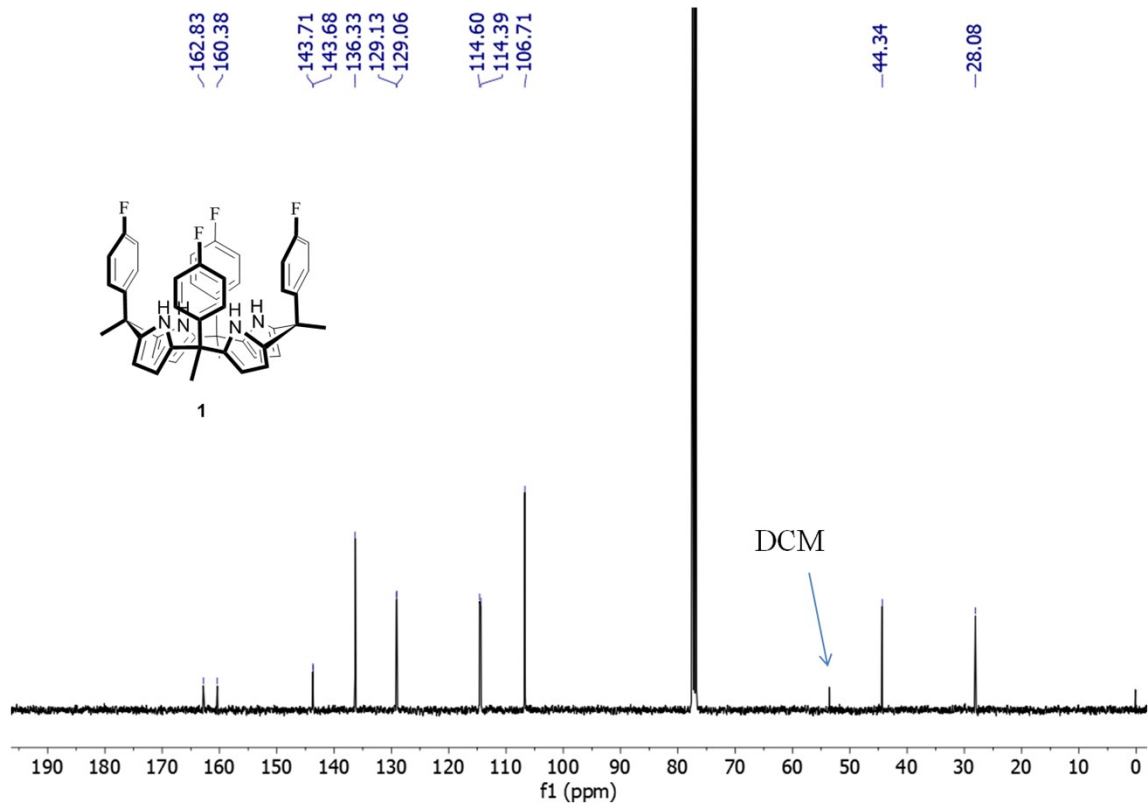


**Figure S2.**  $^{13}\text{C}$  NMR spectrum of **1** in  $\text{CDCl}_3$ .

# Spectrum Plot Report

Name	143_3	Rack Pos.		Instrument	Instrument 1	Operator	
Inj. Vol. (ul)	5	Plate Pos.		IRM Status	Success		
Data File	143_3.d	Method (Acq)	Gradient12M.m	Comment		Acq. Time (Local)	12/29/2022 4:40:05 PM (UTC+05:30)

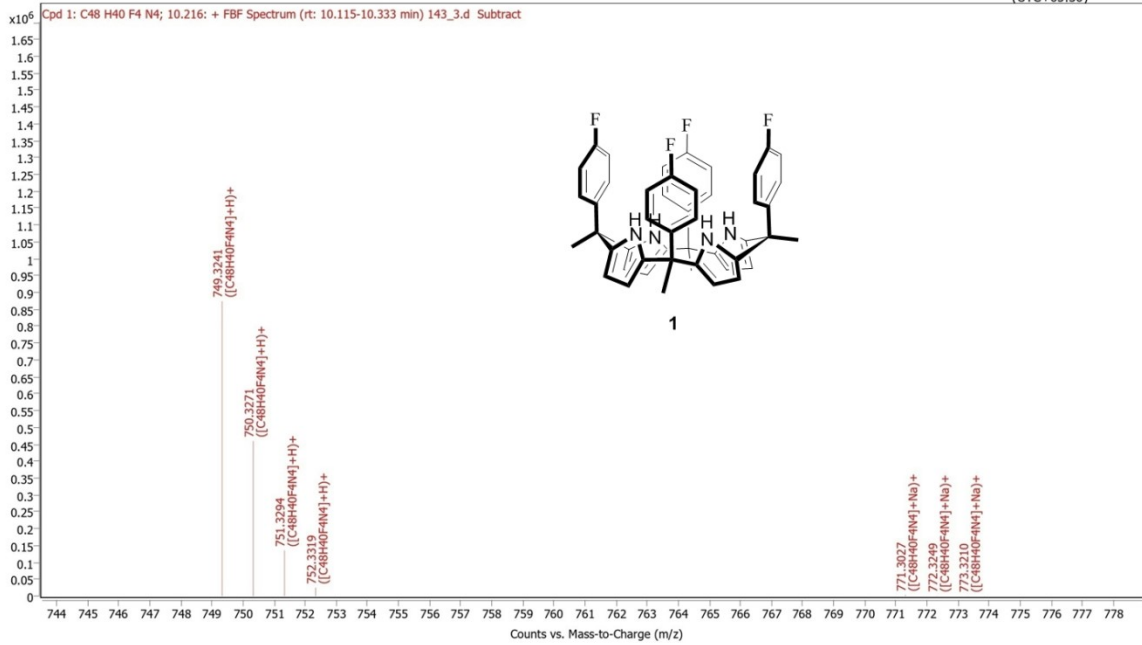


Figure S3. HRMS spectrum of 1

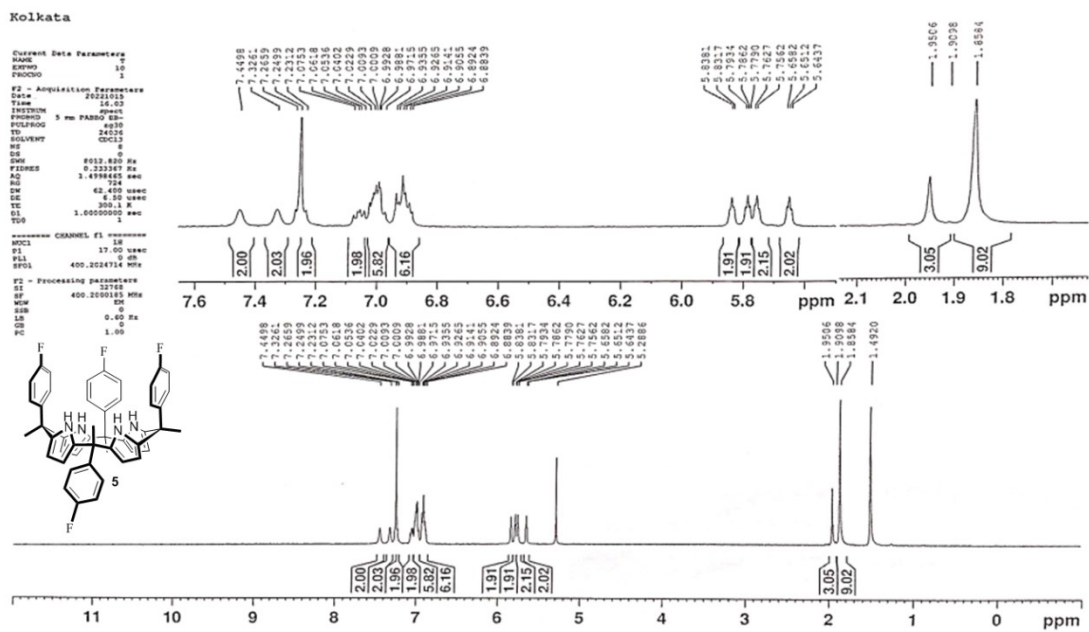
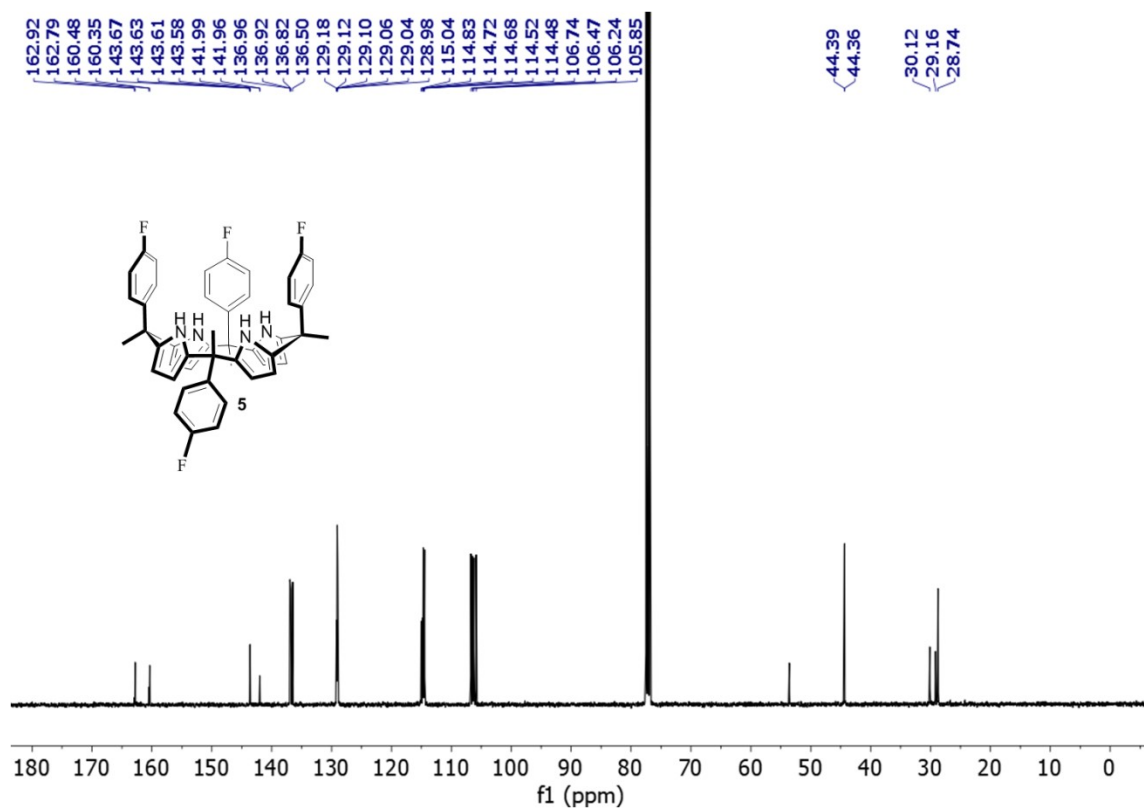


Figure S4.  $^1\text{H}$  NMR spectrum of **5** in  $\text{CDCl}_3$ .





**Figure S5.**  $^{13}\text{C}$  NMR spectrum of **5** in  $\text{CDCl}_3$ .

# Spectrum Plot Report

Name	143_2	Rack Pos.		Instrument	Instrument 1	Operator	
Inj. Vol. (ul)	5	Plate Pos.		IRM Status	Success		
Data File	143_2.d	Method (Acq)	Gradient12M.m	Comment		Acq. Time (Local)	12/29/2022 4:27:17 PM (UTC+05:30)

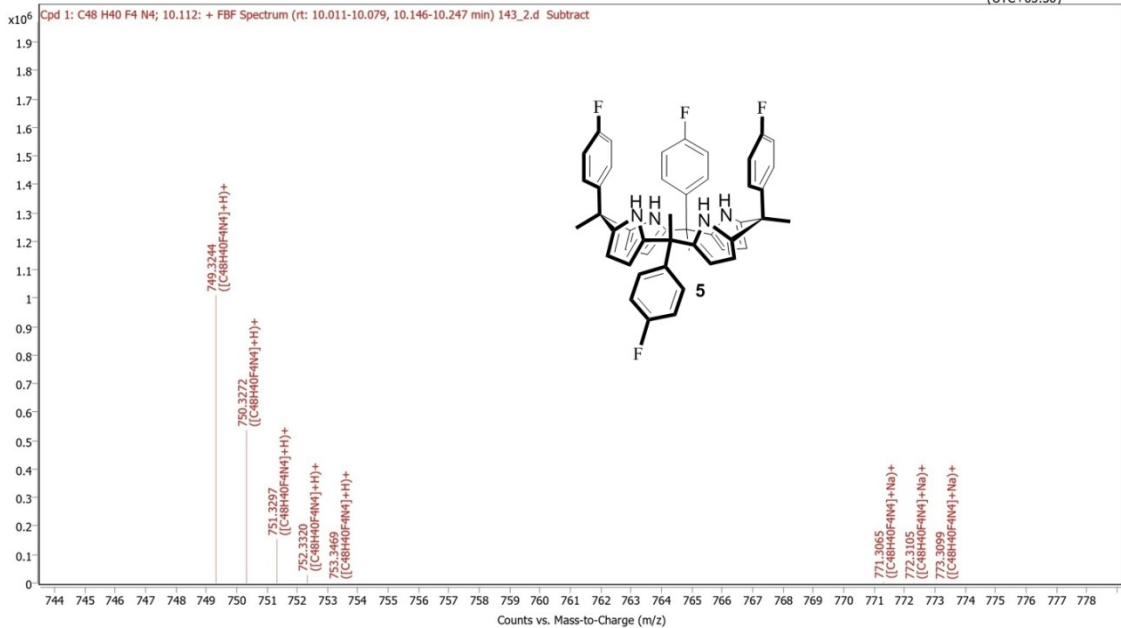


Figure S6. HRMS spectrum of 5.

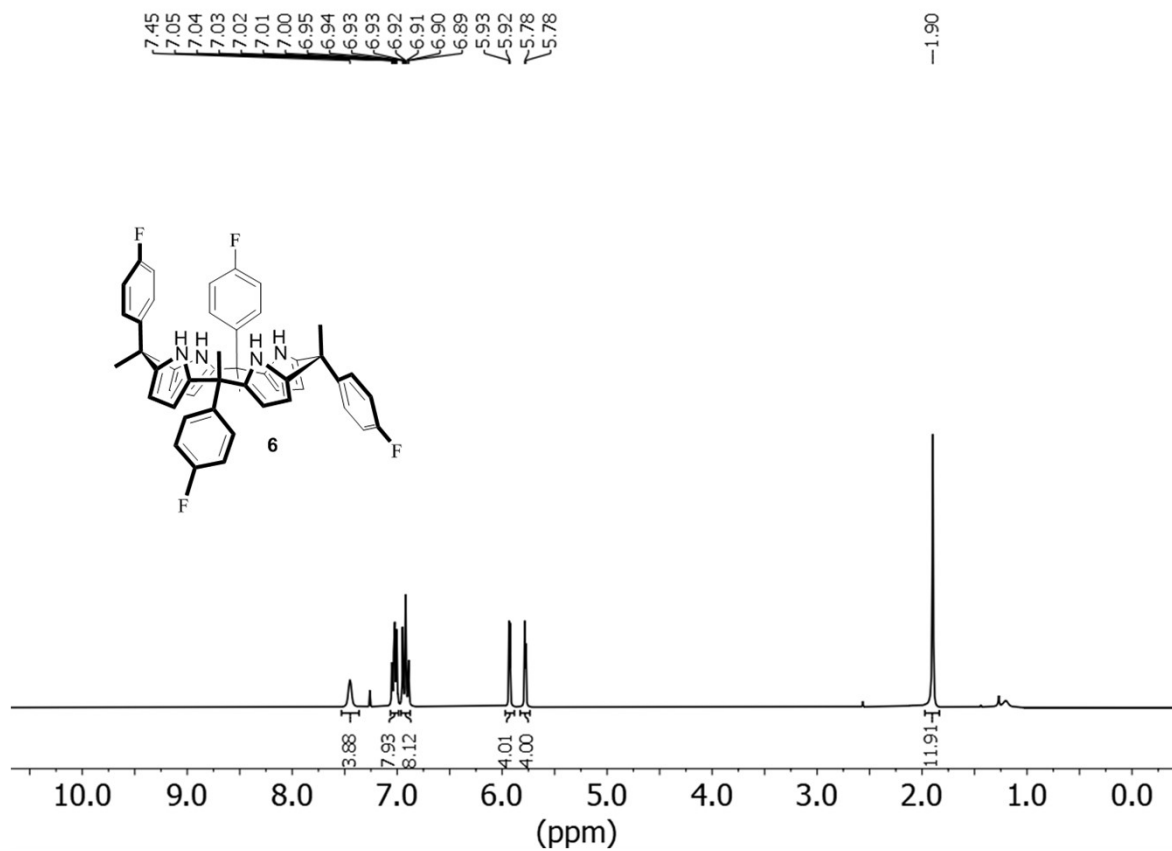
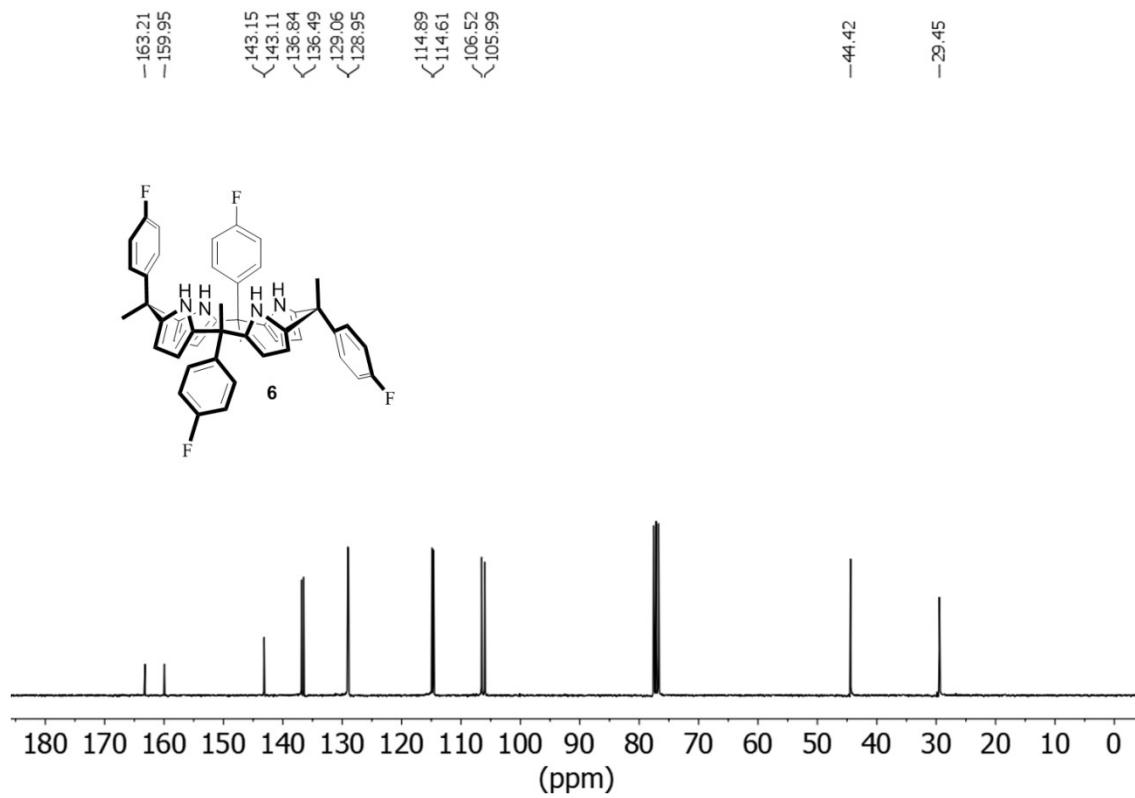
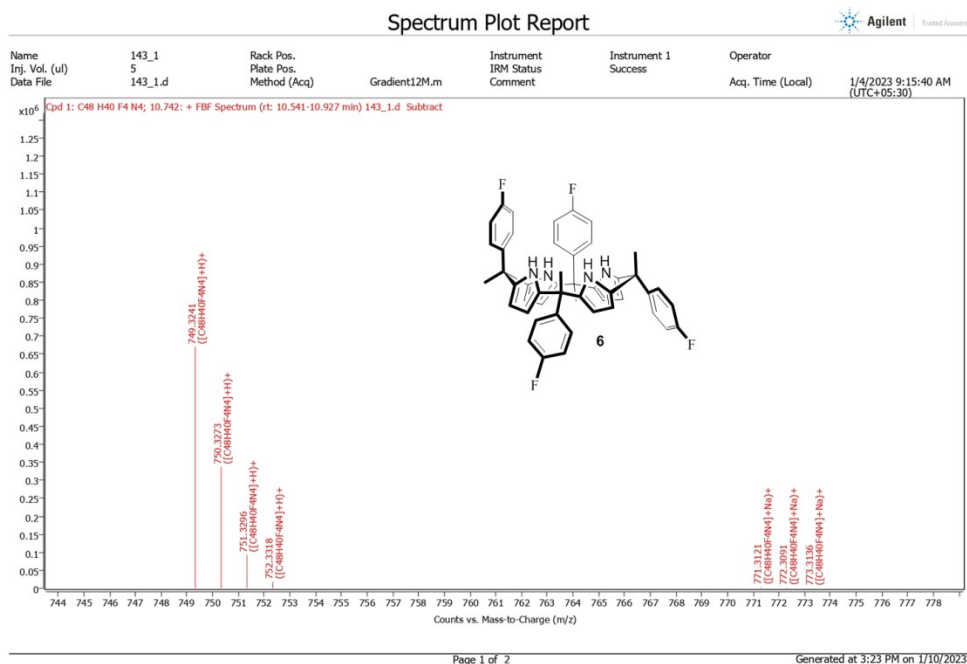


Figure S7. <sup>1</sup>H NMR spectrum of **6** in CDCl<sub>3</sub>.



**Figure S8.**  $^{13}\text{C}$  NMR spectrum of **6** in  $\text{CDCl}_3$ .



**Figure S9.** HRMS spectrum of **6**.

### Section S3. Experimental details for single crystal X-ray structure determination.

#### X-ray experimental for **1**•(CH<sub>3</sub>OH)<sub>2</sub>

Diffraction-grade single crystals of **1**•(CH<sub>3</sub>OH)<sub>2</sub> were obtained as colorless blocks via the slow evaporation of chloroform/ methanol solution (1:1, v/v) of receptor **1**.

#### X-ray experimental for **6**

Diffraction-grade single crystals of **6** were obtained as colorless blocks via the slow evaporation of chloroform/ methanol solution (1: 2, v/v) of compound **6**.

#### X-ray experimental for complex of **1** with cesium fluoride

In a crystal tube methanolic solution of CsF salt was layered over a CHCl<sub>3</sub> solution of receptor **1**. Diffraction-grade single crystals of **1**•CsF•CH<sub>3</sub>OH complex were obtained as colorless needles at the juncture of two layers after few days.

#### X-ray experimental for complex of **1** with tetraethylammonium fluoride

In a crystal tube methanolic solution of TEAF salt was layered over a CHCl<sub>3</sub> solution of receptor **1**. Diffraction-grade single crystals of **1**•TEAF complex were obtained as colorless blocks at the juncture of two layers after few days.

**Table S1.** Selected crystal data and refinement parameters for receptor **1**•(CH<sub>3</sub>OH)<sub>2</sub> and **6**.

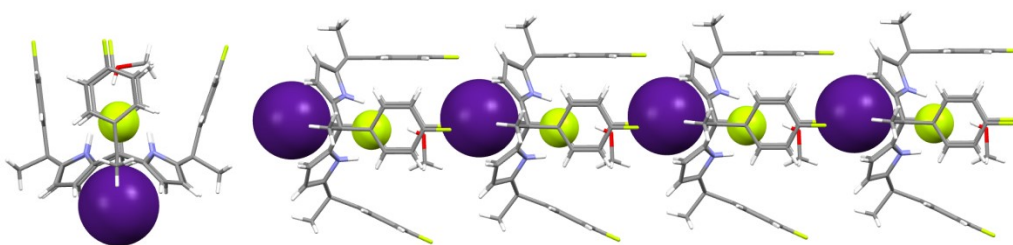
Identification code	<b>1</b> •(CH <sub>3</sub> OH) <sub>2</sub>	<b>6</b>
Empirical formula	C <sub>50</sub> H <sub>46</sub> F <sub>4</sub> N <sub>4</sub> O <sub>2</sub>	C <sub>48</sub> H <sub>40</sub> F <sub>4</sub> N <sub>4</sub>
Formula weight	810.91	748.873
Temperature/K	273.15	273.15
Crystal system	orthorhombic	triclinic
Space group	Pnma	<i>P</i> -1
<i>a</i> /Å	15.116(6)	9.3994(3)
<i>b</i> /Å	22.806(9)	9.7222(4)
<i>c</i> /Å	11.975(4)	11.2104(5)
$\alpha$ /°	90	73.502(2)
$\beta$ /°	90	71.940(2)
$\gamma$ /°	90	84.606(2)
Volume/Å <sup>3</sup>	4128(3)	933.85(7)
<i>Z</i>	4	1
$\rho_{\text{calc}}$ /g/cm <sup>3</sup>	1.305	1.332
$\mu$ /mm <sup>-1</sup>	0.092	0.092
<i>F</i> (000)	1704.0	392.2
Crystal size/mm <sup>3</sup>	0.25 × 0.21 × 0.12	0.4 × 0.2 × 0.1
Radiation	MoK $\alpha$ ( $\lambda$ = 0.71073)	Mo K $\alpha$ ( $\lambda$ = 0.71073)
2 $\theta$ range for data collection/°	4.34 to 50.694	4.36 to 51
Index ranges	-18 ≤ <i>h</i> ≤ 18, -27 ≤ <i>k</i> ≤ 27, -14 ≤ <i>l</i> ≤ 14	-13 ≤ <i>h</i> ≤ 13, -13 ≤ <i>k</i> ≤ 13, -15 ≤ <i>l</i> ≤ 15
Reflections collected	46133	18393
Independent reflections	3877 [ <i>R</i> <sub>int</sub> = 0.0802, <i>R</i> <sub>sigma</sub> = 0.0442]	3481 [ <i>R</i> <sub>int</sub> = 0.0412, <i>R</i> <sub>sigma</sub> = 0.0511]
Data/restraints/parameters	3877/0/284	3481/0/256
Goodness-of-fit on <i>F</i> <sup>2</sup>	1.050	1.078
Final <i>R</i> indexes [ <i>I</i> ≥ 2 $\sigma$ ( <i>I</i> )]	<i>R</i> <sub>1</sub> = 0.0523, <i>wR</i> <sub>2</sub> = 0.1224	<i>R</i> <sub>1</sub> = 0.0413, <i>wR</i> <sub>2</sub> = 0.1028
Final <i>R</i> indexes [all data]	<i>R</i> <sub>1</sub> = 0.0810, <i>wR</i> <sub>2</sub> = 0.1347	<i>R</i> <sub>1</sub> = 0.0603, <i>wR</i> <sub>2</sub> = 0.1097
Largest diff. peak/hole / e Å <sup>-3</sup>	0.49/-0.50	0.27/-0.20
<b>CCDC</b>	<b>2387264</b>	<b>2387266</b>

**Table S2.** Selected crystal data and refinement parameters for **1•CsF•CH<sub>3</sub>OH** and **1•TEAF** complexes.

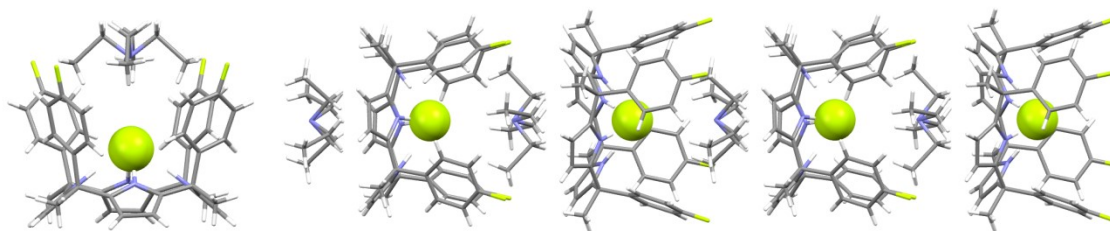
Identification code	<b>1•CsF•CH<sub>3</sub>OH</b>	<b>1•TEAF</b>
Empirical formula	C <sub>49</sub> H <sub>44</sub> CsF <sub>5</sub> N <sub>4</sub> O	C <sub>56</sub> H <sub>60</sub> F <sub>5</sub> N <sub>5</sub>
Formula weight	932.79	898.09
Temperature/K	281.00	281.00
Crystal system	monoclinic	tetragonal
Space group	<i>P2<sub>1</sub>/m</i>	<i>P4/ncc</i>
<i>a</i> /Å	9.6024(3)	15.5418(6)
<i>b</i> /Å	17.3934(5)	15.5418(6)
<i>c</i> /Å	12.9275(4)	19.8506(11)
$\alpha$ /°	90	90
$\beta$ /°	91.6420(10)	90
$\gamma$ /°	90	90
Volume/Å <sup>3</sup>	2158.24(11)	4794.9(5)
Z	2	4
$\rho_{\text{calc}}$ /cm <sup>3</sup>	1.435	1.244
$\mu$ /mm <sup>-1</sup>	0.921	0.087
F(000)	948.0	1904.0
Crystal size/mm <sup>3</sup>	0.6 × 0.3 × 0.1	0.6 × 0.4 × 0.2
Radiation	MoK $\alpha$ ( $\lambda$ = 0.71073)	MoK $\alpha$ ( $\lambda$ = 0.71073)
2 $\theta$ range for data collection/°	4.244 to 50.732	4.87 to 50.776
Index ranges	-11 ≤ <i>h</i> ≤ 11, -19 ≤ <i>k</i> ≤ 20, -15 ≤ <i>l</i> ≤ 15	-18 ≤ <i>h</i> ≤ 18, -18 ≤ <i>k</i> ≤ 18, -23 ≤ <i>l</i> ≤ 23
Reflections collected	39435	62658
Independent reflections	4105 [ <i>R</i> <sub>int</sub> = 0.1018, <i>R</i> <sub>sigma</sub> = 0.0913]	2204 [ <i>R</i> <sub>int</sub> = 0.0917, <i>R</i> <sub>sigma</sub> = 0.0260]
Data/restraints/parameters	4105/0/303	2204/138/176
Goodness-of-fit on <i>F</i> <sup>2</sup>	1.075	1.226
Final <i>R</i> indexes [ <i>I</i> ≥ 2 $\sigma$ ( <i>I</i> )]	<i>R</i> <sub>1</sub> = 0.0722, <i>wR</i> <sub>2</sub> = 0.1424	<i>R</i> <sub>1</sub> = 0.1280, <i>wR</i> <sub>2</sub> = 0.2655
Final <i>R</i> indexes [all data]	<i>R</i> <sub>1</sub> = 0.1383, <i>wR</i> <sub>2</sub> = 0.1612	<i>R</i> <sub>1</sub> = 0.1422, <i>wR</i> <sub>2</sub> = 0.2732
Largest diff. peak/hole / e Å <sup>-3</sup>	1.06/-0.80	0.43/-0.43
<b>CCDC</b>	<b>2387267</b>	<b>2387269</b>

**Table S3.** Selected distances and angles for non-covalent interactions seen in the single crystal X-ray structure of TEAF and CsF complexes of **1**.

Complexes	N-H---A <sup>-</sup> distances (Å)	N---A <sup>-</sup> distances (Å)	<N-H---A <sup>-</sup> angle (°)	Distance(s) between A <sup>-</sup> ---Centroids of phenyl ring (Å)
<b>1</b> •TEAF	1.94	2.753	172.48	4.591
<b>1</b> •CsF•CH <sub>3</sub> OH	2.09	2.777	124.81	4.211
	2.09	2.777	124.81	4.069
	2.14	2.793	122.81	4.211
	2.14	2.793	122.81	4.603

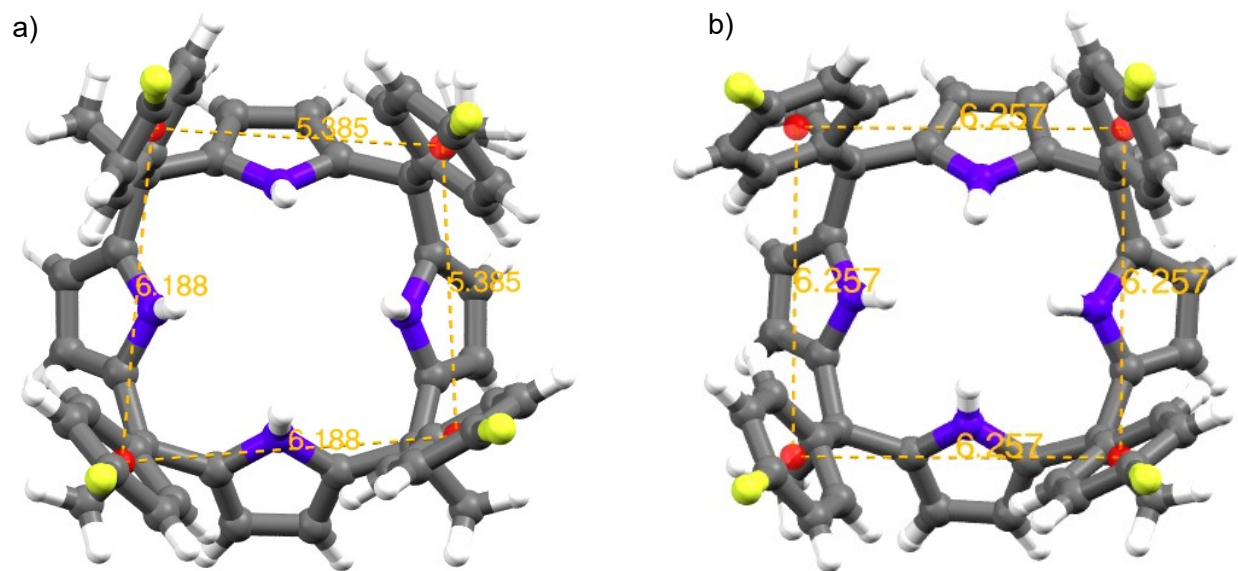


**Figure S10.** Single crystal X-ray structure of **1**•CsF•CH<sub>3</sub>OH complex (left side) and partial view of the 1D linear supramolecular chain seen in the crystal lattice (right side).



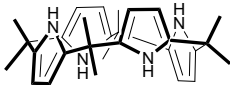
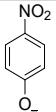
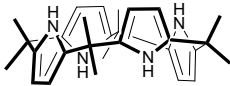
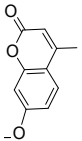
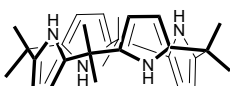
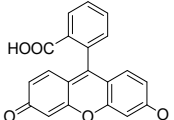
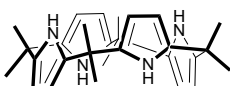
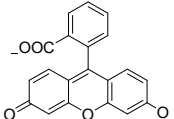
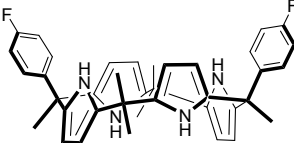
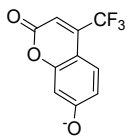
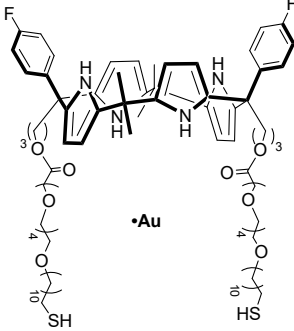
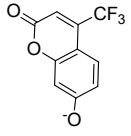
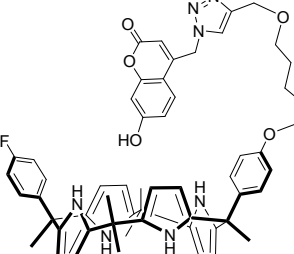
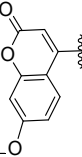
**Figure S11.** Single crystal X-ray structure of **1**•TEAF complex (left side) and partial view of the 1D linear supramolecular chain seen in the crystal lattice (right side).

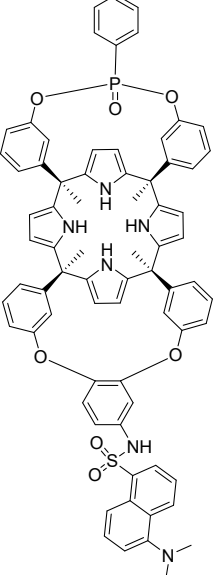
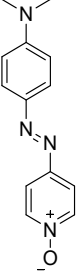
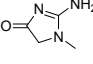
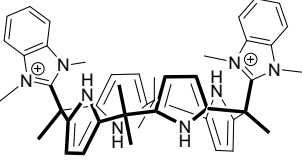
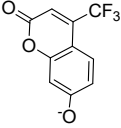
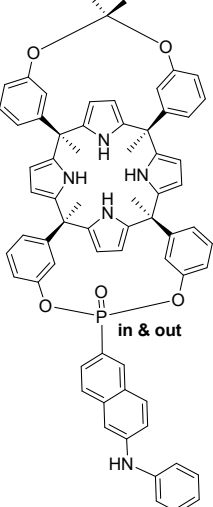
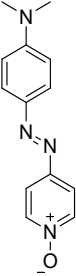
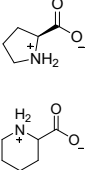
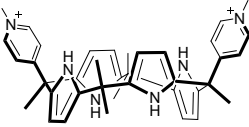
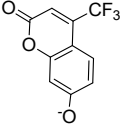




**Figure S12.** Differential arrangement of *meso*-aryl groups in the solid state structures of a) **1**•CsF•CH<sub>3</sub>OH and b) **1**•TEAF complexes. The bound guests are omitted for clarity.

**Table S4.** Some reported IDA/FDDA-based sensors built on calix[4]pyrrole framework for various analytes including fluoride anion.

Host molecule	IDA dye used	Method/ Solvent	Analyte	LOD	References
		UV/CH <sub>2</sub> Cl <sub>2</sub>	F <sup>-</sup>	—	P. A. Gale, P. A. Gale, L. J. Twyman, C. I. Handlin and J. L. Sessler, <i>Chem. Commun. (Camb.)</i> , 1999, 1851–1852.
		Fluorescence/ CH <sub>3</sub> CN	F <sup>-</sup>	67.1 nM	S. Amharar and A. Aydogan, <i>Dyes Pigm.</i> , 2022, <b>197</b> , 109918
		Fluorescence/ CH <sub>3</sub> CN	F <sup>-</sup>	9.1 nM	S. Amharar and A. Aydogan, <i>Dyes Pigm.</i> , 2022, <b>197</b> , 109918
		Fluorescence/ CH <sub>3</sub> CN	F <sup>-</sup>	3.2 nM	S. Amharar and A. Aydogan, <i>Dyes Pigm.</i> , 2022, <b>197</b> , 109918
		Fluorescence/ CH <sub>3</sub> CN	F <sup>-</sup>	2.3 ppb	P. Sökkalingam, J. Yoo, H. Hwang, P. H. Lee, Y. M. Jung and C.-H. Lee, <i>European J. Org. Chem.</i> , 2011, <b>2011</b> , 2911–2915.
		Fluorescence/ CH <sub>2</sub> Cl <sub>2</sub>	F <sup>-</sup>	0.7 nM	P. Sökkalingam, S.-J. Hong, A. Aydogan, J. L. Sessler and C.-H. Lee, <i>Chemistry</i> , 2013, <b>19</b> , 5860–5867.
		Fluorescence/ CH <sub>3</sub> CN	F <sup>-</sup>	0.4 nM	D. Sareen, J. H. Lee, H. Hwang, S. Yoo and C.-H. Lee, <i>Chem. Commun. (Camb.)</i> , 2016, <b>52</b> , 5852–5855.

		Fluorescence/ CHCl <sub>3</sub>		110 nM	A. F. Sierra, D. Hernández-Alonso, M. A. Romero, J. A. González-Delgado, U. Pischel and P. Ballester, <i>J. Am. Chem. Soc.</i> , 2020, <b>142</b> , 4276–4284.
		Fluorescence/ CH <sub>3</sub> CN	HCO <sub>3</sub> <sup>-</sup>	4.0 nM	E.Mulugeta,Q.He,D.Sareen,S.J.Hong,J.H.Oh,V.M.Lynch,J.L.Sessler,S.K.KimandC.H.Lee, <i>Chem</i> ,2017, <b>3</b> ,1008–1020.
		Fluorescence/ CH <sub>2</sub> Cl <sub>2</sub>		—	A. F. Sierra, G. Aragay, G. Peñuelas-Haro and P. Ballester, <i>Org. Chem. Front.</i> , 2021, <b>8</b> , 2402–2412.
		Fluorescence/ CH <sub>3</sub> CN	HP <sub>2</sub> O <sub>7</sub> <sup>3-</sup>	2.0 ppb	P. Sokkalingam, D. S. Kim, H. Hwang, J. L. Sessler and C.-H. Lee, <i>Chem. Sci.</i> , 2012, <b>3</b> , 1819.

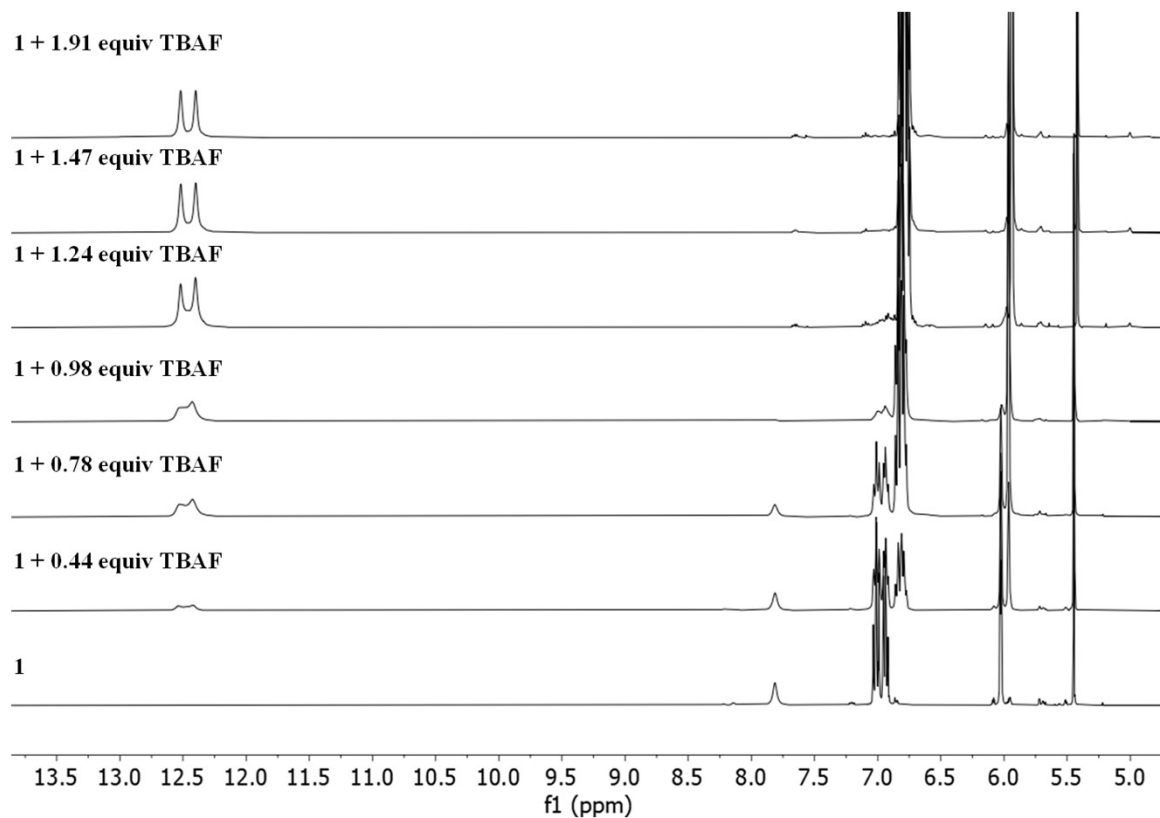


**Figure S13.** Partial  $^1\text{H}$  NMR titration spectra of receptor **1** (1.10 mM) with incremental addition of TBAF in  $\text{CD}_3\text{CN}$ .

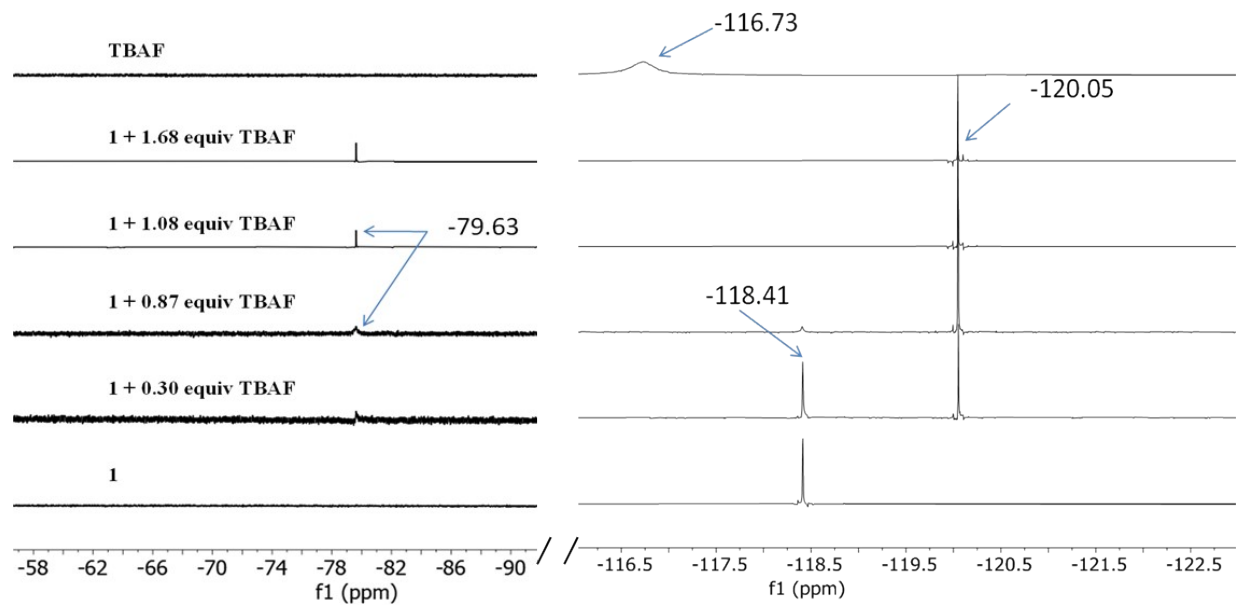


**Figure S14.** Partial  $^{19}\text{F}$  NMR titration spectra of receptor **1** (3.74 mM) with incremental addition of TBAF in  $\text{CD}_3\text{CN}$ .

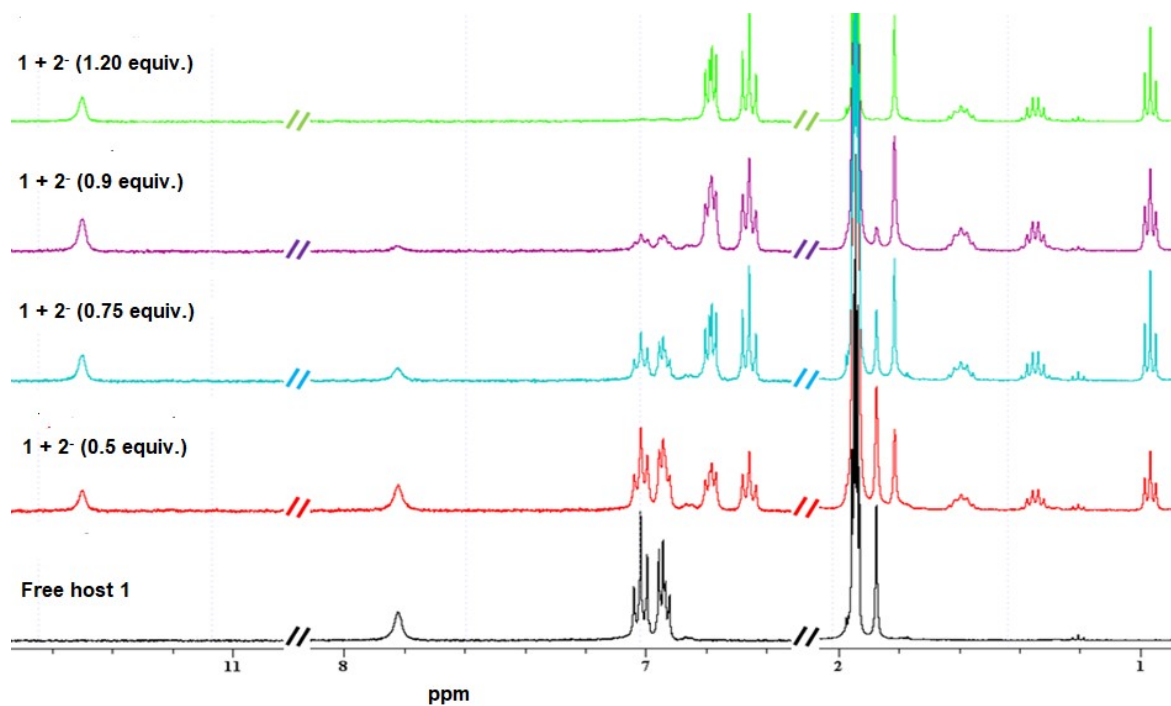


**Figure S15.** Partial <sup>1</sup>H NMR titration spectra of receptor **1** (1.10 mM) with incremental addition of coumarin anion **2<sup>-</sup>** in CD<sub>3</sub>CN. Coumarin anion used as its tetrabutylammonium salt.

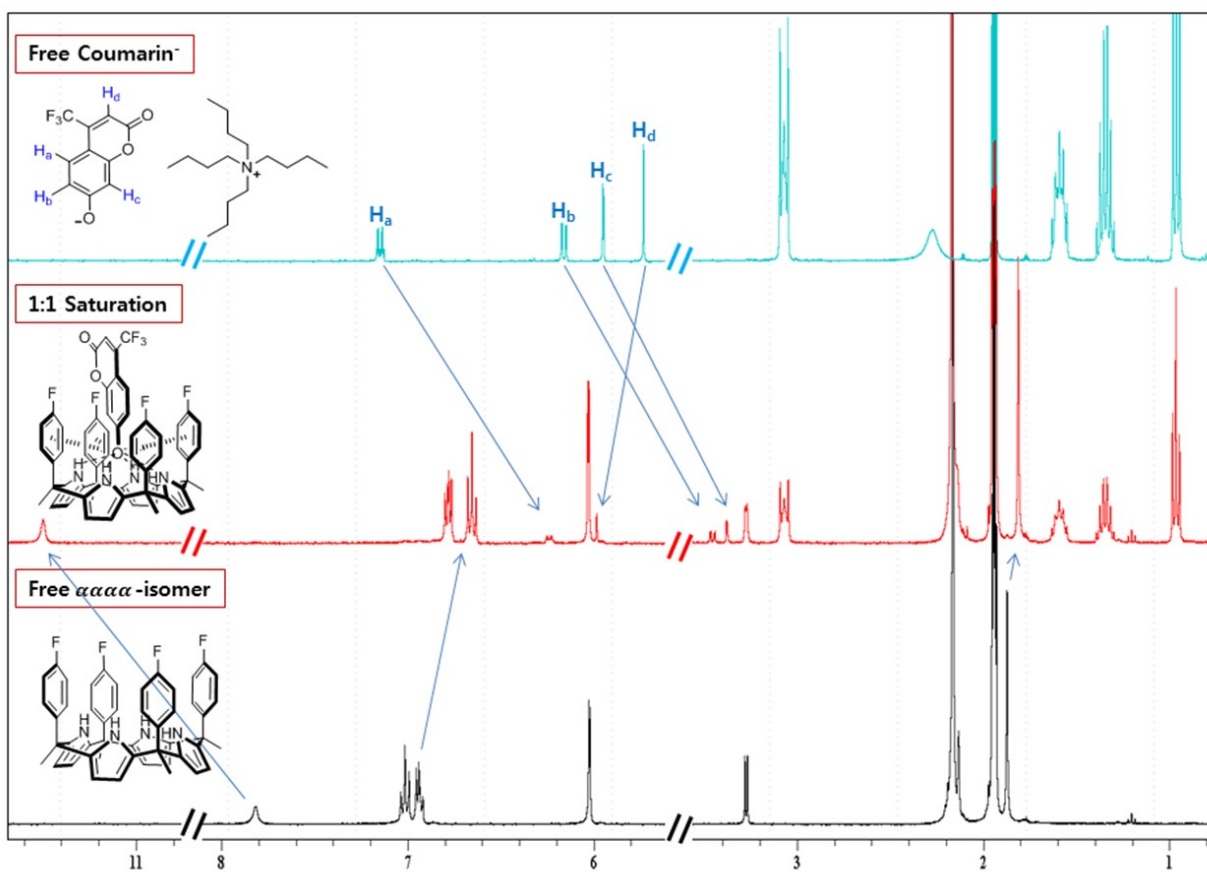


**Figure S16.**  $^1\text{H}$  NMR spectra of **1** ( $1.11 \times 10^{-3}$  M) in the absence and presence of coumarin anion **2<sup>-</sup>** recorded in  $\text{CD}_3\text{CN}$  solution.

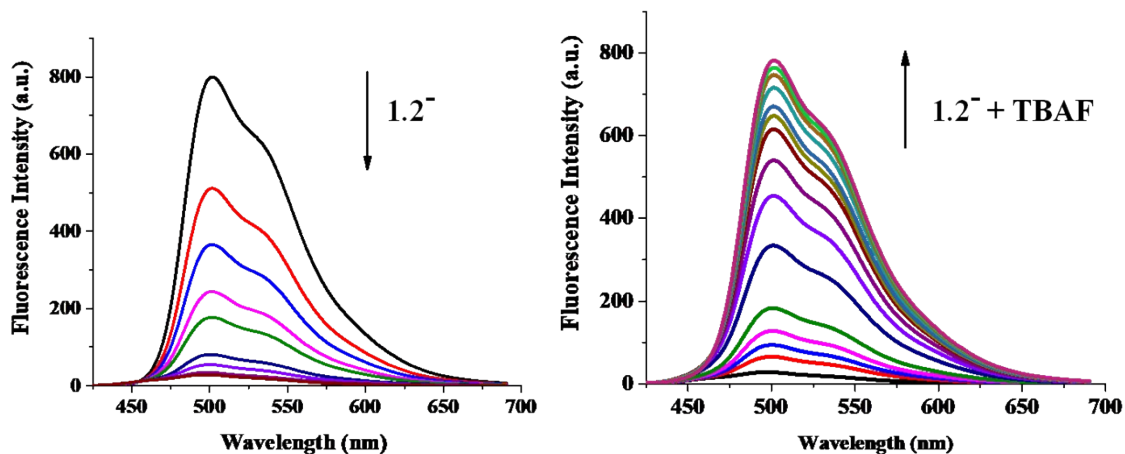


**Figure S17.** Change in fluorescence intensity of  $2^-$  ( $c = 4.0 \times 10^{-6}$  M) upon incremental addition of **1** ( $c = 2.40 \times 10^{-4}$  M, 0-1.0 equivalent) in acetonitrile (left side). Change in fluorescence intensity of  $1 \cdot 2^-$  ( $c = 4 \times 10^{-6}$  M) upon incremental addition of (0 – 4.0 equivalent) TBAF ( $c = 8 \times 10^{-6}$  M) in acetonitrile (right side).

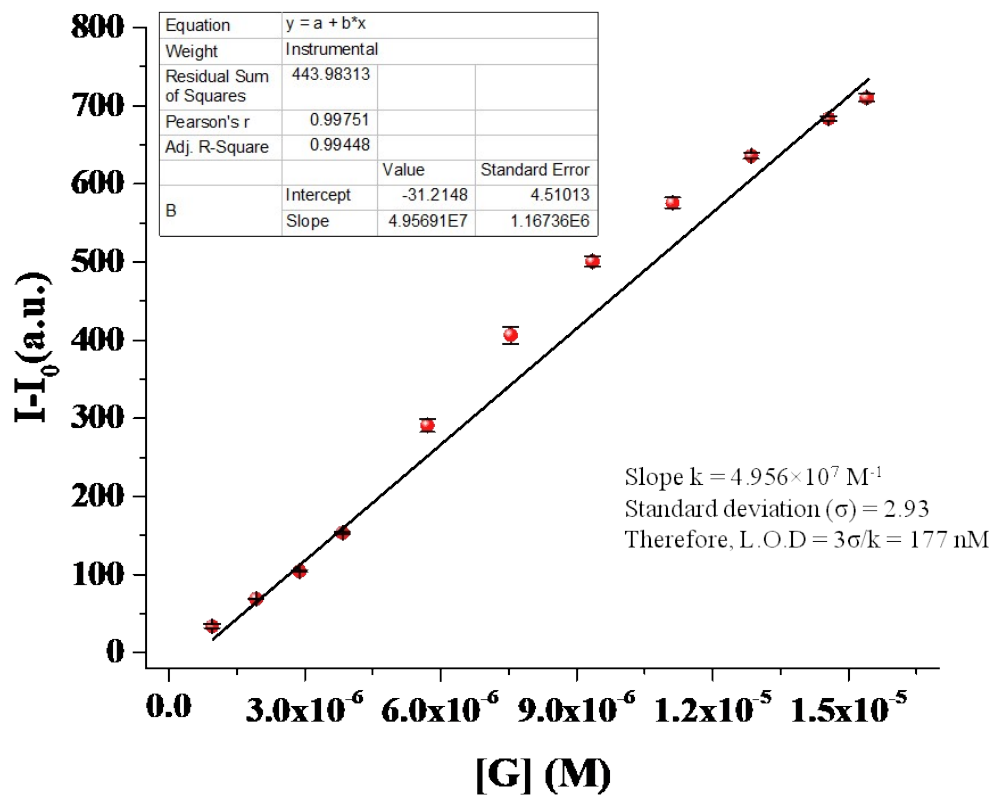


**Figure S18.** Determination of limit of detection (L.O.D) from fluorescence titration of **1.2**<sup>-</sup> with TBAF.



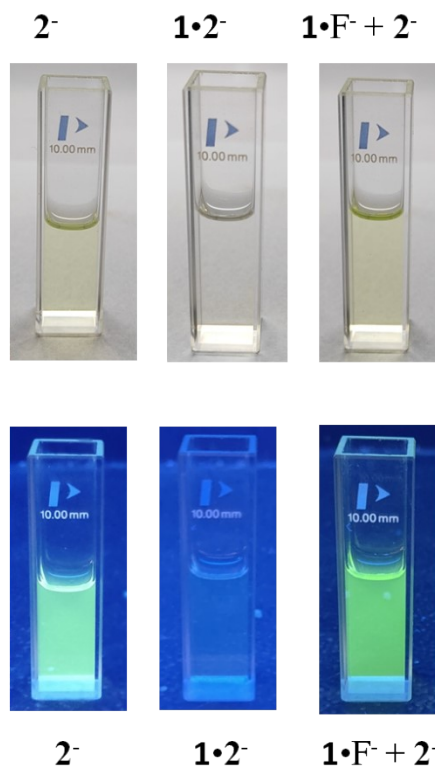


**Figure S19.** Colors of acetonitrile solution of free coumarin anion  $2^-$ ,  $(1 \cdot 2^-)$  complex, and  $1 \cdot F^-$  complex containing decomposed  $2^-$  seen during FDDA assays under sunlight (upper panel) and UV light (lower panel).  $[2^-] = 1.3 \times 10^{-5}$  M.

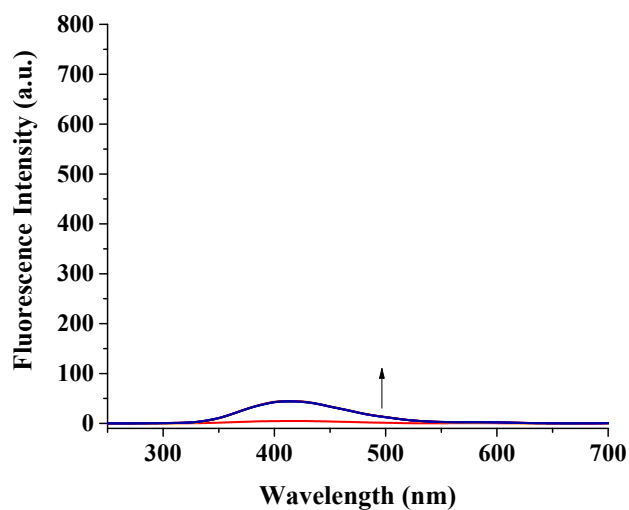


**Figure S20.** Change in fluorescence intensity of **1** ( $c = 6.4 \times 10^{-5}$  M) upon incremental addition of TBAF ( $c = 1.27 \times 10^{-2}$  M, 0-7.0 equivalent) in acetonitrile ( $\lambda_{\text{ex}} = 230$  nm).

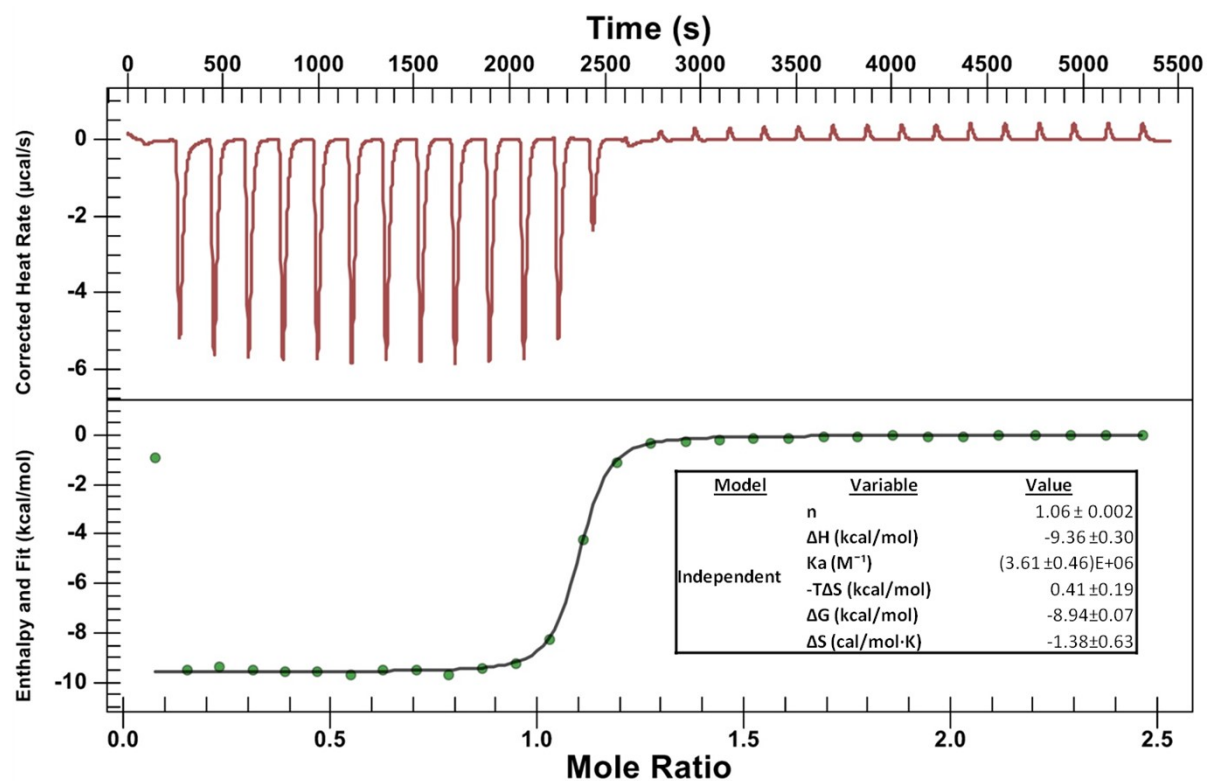


**Figure S21.** ITC plot showing titration of receptor 1 (0.27 mM) with coumarin anion 2<sup>-</sup> in CH<sub>3</sub>CN at 298K.

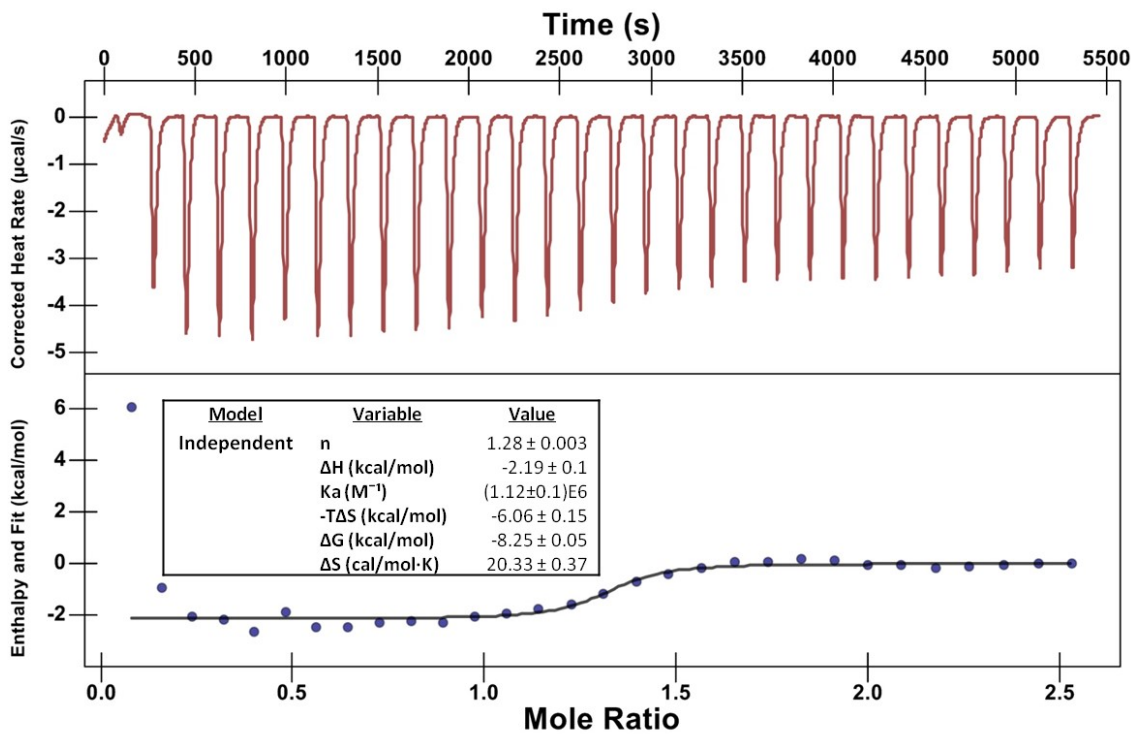


**Figure S22.** ITC plot showing titration of receptor 1 (0.2 mM) with TBAF (3.76 mM) in CH<sub>3</sub>CN at 298K.